Polymer Chemistry

Accepted Manuscript

ROYAL SOCIETY OF CHEMISTRY

www.rsc.org/polymers

Polymer Chemistry

RSC Publishing

ARTICLE

Intracellular redox potential-responsive micelles based on polyethylenimine-cystamine-poly(ε-caprolactone) block copolymer for enhanced miR-34a delivery

Cite this: DOI: 10.1039/x0xx0000x

Received 00th January 2012,
Accepted 00th January 2012

DOI: 10.1039/x0xx00000x

www.rsc.org/

Hanmei Li [a], HaoJiang [a], Mengnan Zhao [a], Yao Fu [a], Xun Sun[a*]

An amphiphilic cationic graft polymer polyethylenimine-cystamine-poly (ε-caprolactone) (PSSP) with intracellular redox potential-responsive cleavable ability was for the first time synthesized by coupling poly (ε-caprolactone) (PCL) to polyethylenimine (PEI) via bio-cleavable disulfide linkage. The PSSP based micelles, which can degrade in the intracellular reducing environment, were developed as smart non-viral gene vectors for enhanced miR-34a delivery. PSSP/miR-34a complexes showed effective and stable miRNA condensation with the narrow particle size around 120 nm. The gel retardation assay showed that PSSP micelles could protect miRNA from RNase and achieved intracellular release of miRNA in the reducing environment. Compared with PEI25K, PSSP revealed comparable transfection efficiencies in B16F10 cell with less cytotoxicity. The B16F10 cell treated with PSSP/miR-34a complexes showed significant higher cell apoptosis than PEI 25K/miR-34a complexes. These encouraging results indicated that the PSSP may possess the promising potential as a smart non-viral gene vector with low cytotoxicity, intracellular redox potential to trigger miRNA release and high transfection efficiency.

Introduction

Gene therapy is a promising treatment for many diseases. Gene carriers play key roles in protecting therapeutic genes from degradation and in the specific presentation of therapeutic genes to the target cells. Non-viral gene vectors presented pronounced advantages over viral vectors due to improved safety and biocompatibility.[1,2] Numerous cationic polymers have been developed for fabricating non-viral carrier systems, e.g., poly-(L-lysine), poly-(ethyleneimine) (PEI) and cationic block copolymers based on these homopolymers, e.g. poly(ethylene glycol)-block-poly-(ethyleneimine).[3-5]

Among various polycations, PEI takes a prominent position due to its potential for endosomal escape and high transfection efficiencies comparable to viral vectors.[6] The gene condensation ability of high molecular weight PEI is better than low molecular weight PEI, but the cytotoxicity of PEI increased with their molecular weight.[2] Therefore, optimizing PEI based gene vector for high gene transfection ability and low cytotoxicity has drawn increasing attentions in the field. Linking low molecular weight PEI to hydrophobic segments to form amphiphilic cationic polymer is an effective strategy.[7] The hydrophobic segments can partially shield the positive charge of PEI, condense DNA into small complexes with particle size of 100 nm and enhance the interactions between polymers and the cell membranes.[8] However, the gene transfection efficiency of this method might be limited due to the tight packing of genes, which is in general preferred for protecting therapeutic genes from enzymatic degradation before reaching the target site.[9] Moreover, tight packing was found to prevent therapeutic genes from reaching the transcription machine after cellular internalization.[10] Therefore, developing PEI based polymeric vector which can deliver genes efficiently to the target site via tight packing of genes and then release genetic materials in the cytoplasm triggered by cellular stimuli should be a good strategy with better gene transfection efficiency. Intracellular pH and redox potential are two commonly investigated cellular stimuli.[11-13] Although pH-responsive polymers can degrade in the acidic environment of endosomes or lysosomes thus resulting in the release of therapeutic genes, the exposure of released therapeutic gene to the endosomes and lysosomes also leads to the reduction of their bioavailability at target sites such as the cytosol and the nucleus.[12, 13] Recent research showed strong gradient is present between reducing sub-cellular compartment and oxidizing extracellular environment,[12] which also can be explored as stimulus for releasing the therapeutic gene. Unlike pH-induced degradation, redox potential can trigger the degradation of redox potential-responsive polymer after them escaped from the endolysosomal compartment and release therapeutic genes in cytosol or the nucleus without degradation in the endolysosomes, leading to better bioavailability than pH-induced degradation.[13, 14]

Micro-RNAs (miRNAs) are a class of small non-coding RNAs which could control gene expression. Increasing evidence indicates that a number of miRNAs possessing tumor-suppressive properties play an important role in human cancer therapy. The miR-34a is one of the most characterized tumor suppressor miRNAs.[15]

Overexpression of miR-34a can cause cell apoptosis and subsequently result in inhibition of cancer regeneration, migration, and metastasis.[16, 17]

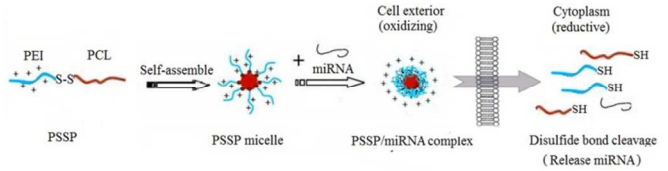

Scheme 1 Schematic illustration of preparation of PSSP based micelles and controlled release of miRNA upon intracellular redox potential stimulus.

In this study, we designed and developed an intracellular redox potential-responsive micellar system for gene delivery. The hydrophobic polymer polycaprolactone (PCL) was grafted on the PEI via a reducible disulfide bond to afford an amphiphilic cationic block copolymer PCL-SS-PEI (PSSP). Subsequently the PSSP based micelles were applied for the delivery of miR-34a (Scheme 1).The micelles could stabilize and protect the payloads before reaching the target site. After escaping from the endolysosomal compartment and reaching the cytoplasm of target cells, miR-34a is expected to be released from the micelles triggered by redox potential of the cytoplasm, which will effectively enhance the anti-cancer efficiency of miR-34a.The PCL-PEI without disulfide bonds (PP) was also synthesized and investigated to compare with PSSP to explore the impact of disulfide bond on the physicochemical properties as well as the miR-34a transfection efficiency of the polymeric vector.

Experimental section

1. Materials

Branched PEI with molecular weights of 2000 (PEI2K) and 25,000 (PEI25K), ε-caprolactone, stannous (II) octoate (SnOct), and cystamine dihydrochloride were obtained from Sigma-Aldrich (USA).ε-caprolactone was purified by vacuum distillation from calcium hydride (CaH_2). 4-nitrophenyl chloroformate (NPC) was obtained from Aladdin (China). Benzyl alcohol and dichloroform were of analytic grade and were distilled before use. Mmu-miR-34a mimics and control miRNA were synthesized by GenePharm (Shanghai, China) and FAM-labeled miRNA was supplied by RiboBio (Guangzhou, China). Other chemicals and reagents were of analytical grade and obtained commercially.

2. Synthesis of polyethylenimine-graft-poly(ε-caprolactone) (PP)

Scheme 2 shows the overall reaction scheme for PP. It consists of three steps including the synthesis of poly(ε-caprolactone) (PCL-OH) (Scheme 2-A), the activation of PCL-OH with NPC (Scheme 2-B) and the coupling of NPC-activated PCL with PEI (Scheme 2-C).

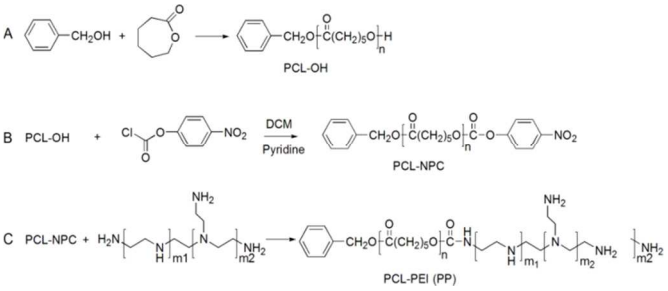

Scheme 2. Synthetic route of PP.

2.1. Synthesis of PCL-OH

Monohydroxy-terminated PCL-OH was first synthesized by ring-opening polymerization of ε-caprolactone using benzyl alcohol as an initiator and SnOct as a catalyst (0.1% moles of ε-caprolactone) according to the literature.[18] In brief, ε-caprolactone (100 mmol, 11.4 g) and benzyl alcohol (10 mmol, 1.08 g) were weighed into a dry round-bottom flask, and 0.1% amount of SnOct was added. Polymerization was carried out in dry nitrogen atmosphere and stirred constantly at 120 ºC for 24 h. Then the product was dissolved in $CH_2Cl_2$and precipitated three times in cold methanol. Finally, the white powder was dried in a vacuum oven for 48 h at 40 ºC. The structure of PCL-OH was verified using ^{1}H NMR (400MHz, $CDCl_3$, ppm): δ7.35(t, 5H, C_6H_5-), 5.17(t, 2H, C_6H_5-CH_2-), 4.04(t, 2H,-CH_2O-), 2.32(t, 2H,-CH_2CO), 1.57(4H, m,-CH_2-), 1.34 (2H, m,-CH_2-).The Mw of PCL-OH synthesized was 2020, which was calculated via the integration ratio of peaks at 5.17 (-CH_2-C_6H_5) with those at 4.04 (-CH_2O-).

2.2. Synthesis of activated PCL

Under a nitrogen atmosphere, to a 10 mL DCM solution of PCL-OH (1.2 g, 0.6 mmol) and pyridine (0.4 g, 0.4 mL, 5 mmol), a solution of NPC (1.2 g, 3 mmol) in 10 mL DCM was added at 0 ºC. Afterwards, the reaction proceeded for 24 h at room temperature. The resulting polymer PCL-NPC was isolated by precipitation in cold diethyl ether and dried in vacuum. The structure of PCL-NPC was verified using (400 MHz, $CDCl_3$, ppm): δ7.4-7.80(4H, $C_6H_4NO_2$), 7.35(t, 5H, C_6H_5-), 5.11(t, 2H, C_6H_5-CH_2-), 4.16(t, 2H, -$CH_2COOC_6H_4NO_2$), 4.04(t, 2H,-CH_2OH), 2.32(t, 2H,-CH2CO), 1.57(4H, m,-CH2-), 1.34 (2H, m,-CH2-). The new peak at δ 7.4-7.8 belonged to the benzene ring of NPC, confirming that PCL-NPC was successfully synthesized.

2.3. Synthesis of PP

Under a nitrogen atmosphere, 2mL tetrahydrofuran (THF) solution of PCL-NPC (0.2 g, 0.1 mmol) was dropped into 5mL DMSO solution of PEI2K (1 g, 0.5 mmol) by a dosing device with a rate of 0.25 mL/h. Afterwards, the reaction was stirred for another 24 h at room temperature. Then the reaction solution was transferred into a dialysis tube (Molecular cut-off 8000-14,000 Da) and dialyzed against water for 24 h. PP was collected as a yellow solid after freeze-drying (yield: 49%). The structure of PP was verified using ^{1}H NMR. The ^{1}H NMR spectrum showed that the new peaks at δ 2.7-3.1 ppm belonged to methylene units of PEI. This confirmed the successful synthesis of PP.

3. Synthesis of polyethylenimine-Cystamine-poly(ε-caprolactone) (PSSP)

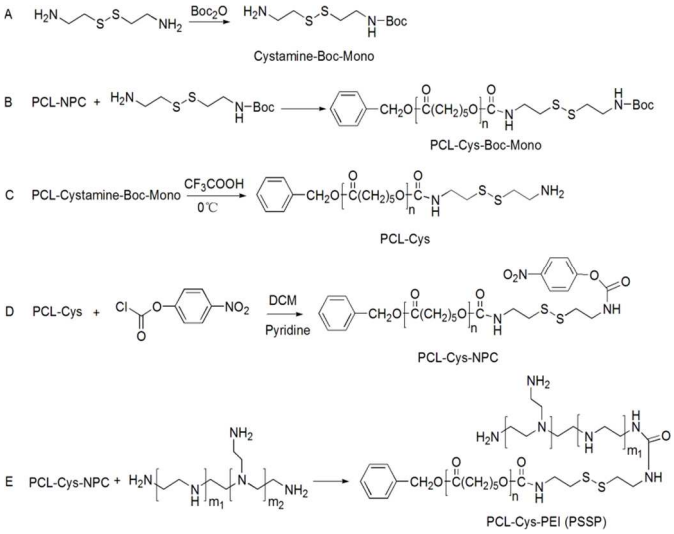

Scheme3. Synthetic route of PSSP.

Scheme 3 shows the overall reaction process for PSSP. It consists of several steps including the synthesis of Mono-Boc-cystamine (Scheme 3-A), the synthesis of PCL-Cys-Bon-Mono (Scheme 3-B), the deprotection of PCL-Cys-Boc-Mono (Scheme3-C), the synthesis of PCL-Cys-NPC (Scheme3-D) and the synthesis of PSSP (Scheme3-E).

3.1. Synthesis of Cystamine-Boc-Mono

Firstly, cystamine dihydrochloride (2.25 g, 10 mmol) and triethylamine (4 mL, 30 mmol) were added into a flask and dissolved in 20 mL methanol. After 10 minutes, 10 mL methanol solution of Boc_2O (2.18 g, 10 mmol) was added slowly into the above reaction solution at 0 ºC. The mixture was stirred at room temperature in the dark under nitrogen atmosphere for 6 h. The solvent was removed in vacuum and the residue was dissolved in 10 mL water. After that, 30 mL of 1 mol/L NaH_2PO_4 (pH4.2) was added, and the mixture was extracted with 30 mL ether three times to remove the byproduct. The aqueous layer was then basified by adjusting its pH to 10.0 by 1 mol/L NaOH solution and extracted by EtOAc (20 mL ×6). Subsequently the organic layer was dried with anhydrous Na_2SO_4 and evaporated to obtain yellow viscous syrup. The reaction yield was about 43%. The structure of Cystamine-Boc-Mono was verified using ^{1}H NMR (400 MHz, D_2O, ppm) (Fig. 1-A): δ4.96 (s, 1H, NH), 3.47 (q, 2H, CH_2N), 3.07(q, 2 H, CH_2N), 2.82 (t, 4H, CH_2S), 1.52 (s, 2H, NH_2), 1.45 (s, 9H, t-BuO). The new peaks appearing at δ 1.45 belonged to the methyl of Boc, which demonstrated that Cystamine-Boc-Mono was successfully synthesized.

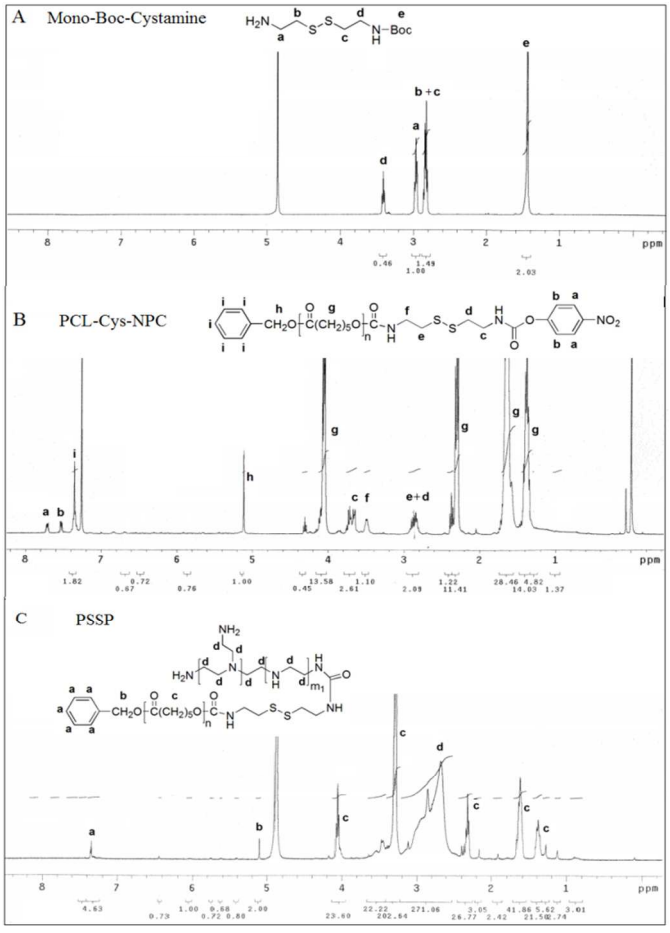

Fig.1. The ^{1}H NMR spectrum of Cystamine-Boc-Mono in D_2O (A), PCL-Cys-NPC in $CDCl_3$(B) and PSSP in $CDCl_3$ (C).

3.2. Synthesis of PCL-Cys-Boc-Mono

PCL-NPC (1 g, 0.5 mmol), Cystamine-Boc-Mono (0.25 g, 1 mmol) and triethylamine (0.5 mL) were dissolved in 10 mL dry CH_2Cl_2 and stirred under a nitrogen atmosphere for one day. Then the solution was filtered, condensed and precipitated in cold methanol to obtain polymer powder PCL-Cys-Boc-Mono. The reaction yield was over 70%. The structure of PCL-Cys-Boc-Mono was verified using ^{1}H NMR. The new peaks appearing at δ 1.45 and 2.5-3.95 belonged to the methyl of Boc and the methylene units of cystamine. At the same time, the peaks at δ 7.4-7.8 belonged to the benzene ring of NPC disappeared. This confirmed that PCL-Cys-Boc-Mono was successfully synthesized.

3.3. Deprotection of PCL-Cys-Boc-Mono

To a 25 mL CH_2Cl_2 solution of polymer PCL-Cys-Boc-Mono (600 mg, 0.3 mmol), 5 mL CF_3COOH was added. After stirred at ice bath for 15 min, CH_2Cl_2 and CF_3COOH were removed by evaporating at reduced pressure. 10 mL of methanol was added and evaporated to totally remove the trifluoroacetic acid. The resulting polymer PCL-Cys-NH_2 was isolated by precipitation in cold diethyl ether and dried in vacuum. The reaction yield was over 62%. The structure of PCL-Cys-NH_2 was verified using ^{1}H NMR. The peaks at δ 1.45 belonged to the methyl of Boc disappear, indicating that PCL-Cys-Boc-Mono was successfully deprotected.

3.4. The Synthesis of PCL-Cys-NPC

Under a nitrogen atmosphere, to a 10 mL DCM solution of PCL-Cys-NH_2 (0.4 g, 0.2 mmol) and pyridine (0.5 mL), a solution of NPC (0.2 g, 1 mmol) in 10 mL DCM was added at 0 ºC. Afterwards, the reaction solution was stirred at room temperature for 24 h. The resulting polymer PCL-Cys-NPC was isolated by precipitation in cold diethyl ether and dried in vacuum. After that, white solid powder PCL-Cys-NPC was obtained with a reaction yield over 73%. The structure of PCL-Cys-NPC was verified using ^{1}H NMR (Fig.1-B). The new peak at δ 7.4-7.8 belonged to the benzene ring of NPC. This confirmed that PCL-Cys-NPC was successfully synthesized.

3.5. The synthesis of PSSP

Under a nitrogen atmosphere, 2 mL THF solution of PCL-Cys-NPC (0.2g, 0.1mmol) was dropped into 5 mL DMSO solution of PEI2K (1g, 0.5mmol) by a dosing device with a rate of 0.25 mL/h. Afterwards, the mixture was stirred at room temperature for another 24 h. Then, the reaction solution was transferred into a dialysis tube (Molecular cut-off 8000-14000 Da) and dialyzed against distilled water for 24 h. After lyophilized, yellow solid was obtained with yield about 30%. The chemical structure of PSSP was identified by ^{1}HNMR spectroscopy. The molecular weight of PP and PSSP were determined by gel permeation chromatography (GPC) relative to a series of low polydispersity PEG standards. GPC measurements were performed using a Waters1515 pump and a Waters 2414 differential refractive index detector. The eluent was 0.1 M NaAc and 0.2 M HAc aqueous solution (pH 5.0) at a flow rate of 1.0 mL/min.

4. Preparation of miRNA loaded polymeric micelle.

Self-assembled polymeric micelles were prepared by solvent evaporation method. Briefly, 10 mg of PP or PSSP copolymer were dissolved in 1 mL THF, and then added dropwise to 10 mL of ultrapurified water. The mixture was stirred for 30 min at room temperature, followed by removing THF and excess water under reduced pressure to adjust the volume to 2 mL for further experiments.

For miRNA loading, polymeric micelles were diluted to different concentrations for desired PEI/miRNA (N/P) ratios using water and added to miRNA solution (80 μg/mL). The mixture was mixed by pipetting and allowed to stand for 15 min before characterization and experiments.

5. Characterization of PP and PSSP micelles **with or without miRNA loading**

The size distribution and zeta potential of polymeric micelle in aqueous solution were measured by dynamic light scattering (DLS) using a Zetasizer Nano ZS90 (Malvern instruments Ltd., UK). The morphology of polymeric micelles or miRNA loaded polymeric micelles was observed under transmission electronmicroscopy (TEM). Samples were dispersed onto a copper grid and then stained with phosphotungstic acid (1%) for 20 s before observation by a TEM instrument (H-600, Hitachi, Japan). Critical micellization concentration (CMC) of the micelles were determined by fluorescence technique using pyrene as the probe as described previously[19]. Briefly, a known amount of pyrene in THF was added to 10 mL volumetric flasks and the solvent was evaporated at 37°C. Subsequently 10 mL of various concentrations of aqueous polymer solutions were added to each volumetric flask and then heated at 37°C for 24 h to equilibrate pyrene with the micelles. The final concentration of pyrene was 6.0×10^{-7} M. Steady-state fluorescent spectra were measured using a fluorescence spectrophotometer (RF-5301 PC, Shimadzu, Kyoto, Japan) at room temperature. For fluorescence emission spectra, excitation wavelength was set at 333 nm and 338nm, respectively.

6. Gel retardation assays.

Condensations of miRNA with PP and PSSP micelles were monitored by a gel electrophoresis assay. 20 μL of formed polymer/miRNA complexes with different N/P ratios were mixed with 4 μL of 6×loading dye and then loaded into a 1% agarose gel containing ethidiumomide (500 ng/mL). Electrophoresis was set up in TAE (Tris-acetate-EDTA) buffer at 120 mV and kept for 15 min. Uncomplexed miRNA or exposed miRNA in the complexes could be detected with a UV illuminator.

To assess the protection effect of PP and PSSP micelles on miRNA against RNase degradation, RNase (1 mU, Sigma, USA) was incubated with miRNA (50 pmol) alone or miRNA complexed with polymer. After 6h, sodium dodecyl sulfate (final concentration=1%) was added and the mixture was denatured at 70 °C for 10 min. Then, miRNA was released from polymer/miRNA complexes by addition of heparin (final concentration = 2%) and the samples were analyzed by electrophoresis on a 1% agarose gel. miRNA band was visualized under UV light.

In addition, to evaluate thiol-triggering miRNA exposure or release from polymer/miRNA complexes, the complexes were exposed to PBS containing 20 mM DTT (Dithiothreitol) and low concentrations (50 μg/mL or 100 μg/mL) of heparin at 37°C for 6h. Then, the mixtures were subjected to electrophoresis.

7. The stability of polymeric micelles in reducing environment.

To assess the stability of PP and PSSP micelles in reducing environment, prepared micelles were added to PBS with or without 20 mM DTT and incubated at 37 °C for specified times. Then, size distributions of the micelles were measured by DLS.

8. Cell uptake assay.

The cellular internalization of PP and PSSP micelles was quantified by flow cytometry. B16F10 cells were maintained in RPMI 1640 supplemented with 10% fetal bovine serum, 100 U/mL penicillin and 100 μg/ml streptomycin. B16F10 cells were seeded on 12-well culture plates 24 h before treated with FITC-labled miRNA (FAM-miRNA) complexed with various polymers. After 4h of treatment, Cells were then washed with PBS containing 20U/ml of heparin and then digested in trypsin for suspension. After washed with PBS for 3 times, cells were analyzed by the Cytomics FC500 flow cytometer (Beckman Coulter, USA).

The cellular uptake of PP and PSSP micelles was also visualized by confocal microscopy. Cells were seeded on coverslips in 12 well culture plate 1 day before treated with Cy3-labeled miRNA complexed with FITC-labeled PP or PSSP in serum-free medium for 4 h. N/P ratio of PEI/miRNA polyplexes were 15/1. The concentration of Cy3-labeled miRNA added to the medium was 2 μg/mL. After incubation, the original medium was removed. Cells were then washed three times with PBS containing 20 U/ml of heparin and fixed in 4% paraformaldehyde. Thereafter, samples were stained with 4'6-diamidino-2-phenylindole (DAPI) for 5min and observed using a Leica TCS SP5 AOBS Confocal microscopy system (Leica, Germany).

9. Cell Viability Assay

B16F10 cells were seeded on 96-well culture plate. 24 h after treated with various concentration of polymers, cell viability was assessed by the MTT method (n=5). Briefly, 10 μL 5mg/ml of MTT (final concentration= 0.5 μg/mL) was added into each well and incubated for 4 h at 37 °C. Then the supernatant was carefully removed and added 150 μL of dimethyl sulfoxide (DMSO) to dissolve the formazan crystals. After incubation at 37 °C for 30 min, absorbance at 570 nm was measured. Cells treated with vehicle were used as control with 100% viability.

10. Assessment of Cell Proliferation and Apoptosis.

Cell proliferation of drug-treated cells was determined by MTT assay. The B16F10 cells were plated in 96-well culture plates for 24 h. Thereafter, cells were transfected with miR-34a complexed with various polymer (2 μg/mL of miR-34a, the N/P of PEI/miR-34a=15/1) for 4 h. After transfection, B16F10 cells were cultured with fresh complete medium for a further 72 h. The cell viability was assayed by MTT method described above.

Cell apoptosis was assayed by 4'6-diamidino-2-phenylindole (DAPI) staining.[20, 21] B16F10 cells were treated with miR-34a complexed with various polymers and replaced with fresh medium after 4 h transfection. Cells were cultured for 72 h and then fixed in 4% paraformaldehyde for 5 min. The cell nuclei were then stained with DAPI for 5 minutes at a final concentration of 1 μg/mL. The cell nucleus morphology was observed under a Zeiss fluorescence microscope (excitation wavelength 358 nm, emission wavelength 461 nm). Cells were judged to be apoptotic or not based on the nucleus morphological changes including chromatin condensation, fragmentation and apoptotic body formation.[20]

Cell apoptosis induction by miR-34a was also quantified by double staining with FITC-Annexin V and propidium iodide (PI) by using the cell apoptotic analysis kit (BD, USA) following the manufacturer's instructions. Flow cytometry were used for quantification of apoptotic cells (n = 3).

11. Statistical analysis

All data were presented as the mean ± standard deviation (SD). Statistical significance was determined by Student's t-test when compared between groups, and comparisons among means of more than two groups were determined by one-way ANOVA. The value of $p < 0.05$ was considered to be statistically significant.

Results and discussion

The PP was synthesized and investigated in comparing with PSSP. PP was synthesized by conjugating NPC functionalized PCL to the amino groups of PEI (Mw = 2000). The detailed synthesis procedures were shown in the Scheme 2. The synthesis of PSSP consisted of several steps including the synthesis of Mono-Boc-cystamine, the synthesis of PCL-Cys-Bon-Mono, the deprotection of PCL-Cys-Boc-Mono, the synthesis of PCL-Cys-NPC and the synthesis of PSSP. Scheme 3 showed the overall reaction process for PSSP. The obtained PSSP was purified by dialysis in distilled water and lyophilized. There are two key steps for the PSSP synthesis. One is the deprotection of PCL-Cys-Boc-Mono (Scheme3-C), low temperature and short reaction time was needed to avoid byproduct. Another step worth noticing was the reaction of PEI with PCL-Cys-NPC (Scheme 3-E). The DMF solution of PCL-Cys-NPC must be added slowly into the DMSO solution of PEI. Otherwise, the graft ratio of PCL on PEI would be too large and generated poorly insoluble copolymer.

Table1. Characteristics of PP and PSSP.

Polymer	Mw of PCL (Da)	Graft ratio	Theory Mw	Experiment Mw
PP	2020	1.30	4626	4932
PSSP	2020	1.34	4707	5039

Mw of PCL: The molecular weight of PCL-OH calculated from ^{1}H NMR spectra.

Graft ratio: The graft ratio calculated from ^{1}H NMR spectra.

Theory Mw: Mw calculated from graft ratio.

Experimental Mw: Mw obtained from GPC analysis.

PSSP was characterized by GPC and ^{1}H NMR analysis. From ^{1}HNMR spectroscopy of PSSP (Fig. 1-C), it can be seen that the peaks at 2.7-3.1 belonged to PEI2K, indicating the successfully synthesis of PSSP. The graft ratio defined as the number of PCL chains per PEI molecule, could be determined from the ratio of the peak area of methylene group in the PCL block to that of the methylene group in the PEI. As shown in Table 1, the graft ratio of PP and PSSP were 1.3 and 1.34, suggesting that almost one PCL was grafted onto one PEI molecule. The Mw of PP and PSSP could be calculated through the graft ratio and these calculated Mw were close to the Mw measured by GPC (Table 1).

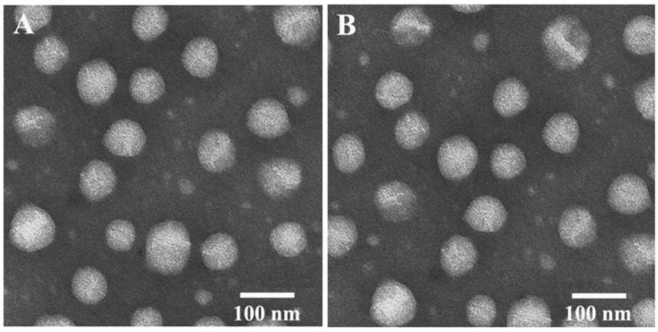

Fig.2. TEM images of PP micelles (A) and PSSP micelles (B).

The PP and PSSP micelles were prepared by solvent evaporation method and characterized by means of DLS and TEM.As shown in Fig. 2, PP and PSSP formed the nearly spherical micelles with an average diameter of about 100 nm.

CMC of the PP and PSSP were determined by a fluorescence technique using pyrene as a probe. In the presence of micelles, pyrene preferentially partitioned into non-polar region of the micelle interior core with a concurrent change in the molecule's photophysical properties. Thus, the excitation spectrum of the pyrene showed a red shift when the PP or PSSP concentration increased and the CMC of them could be estimated based on this photophysical property. The plots of the intensity ratio I_{338}/I_{333} are shown in Fig.S1 as a function of the PP or PSSP concentration. According to previous report[19], pyrene molecules could transfer from apolar to a more hydrophobic microdomain and led to an increase of I_{338}/ I_{333} ratio value. It can be seen from Fig.S1 that the plot of I_{338}/ I_{333} vs. logC is a sigmoidal curve. The CMC was cross-point of the line drawn through the points at the lowest polymer concentrations and another line drawn through the points along the rapidly rising part of the plot. The CMC of PP and PSSP were 8.23 and 7.77 μg/mL, respectively, demonstrating that the introduction of disulfide bond had no obvious influence on the micellar properties of PP.

For miRNA loading, PP and PSSP micelles were mixed with miRNA solution and allowed to stand for 15 min at room temperature. Hydrodynamic diameters and zeta potentials of the polymer/miRNA complexes at various N/P ratios measured by DLS were listed in Table S1. All blank polymer micelles and the polymer/miRNA complexes presented positive charge, indicating that excessive positively charged PEI covered the surface of polymer/miRNA complexes.

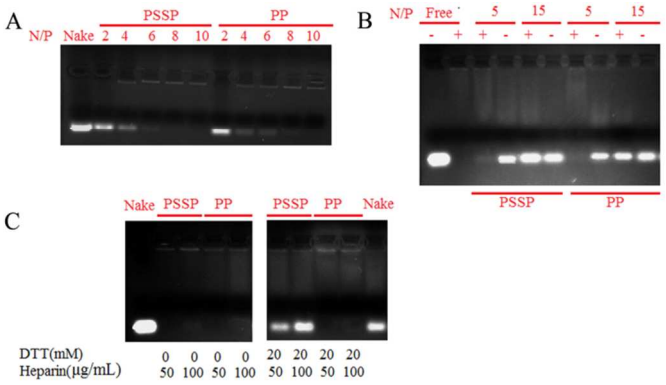

Fig.3. Gel retardation assays. A. Electrophoretic mobility of miRNA in agarose gel after complexed with PP or PSSP micelles at various N/P ratios. B. RNase protection assay. Polymer/complexes were prepared at the N/P ratios of 5 and 10. The "-" represent samples treated with PBS and the "+" represent samples treated with RNase. C. DTT-triggering miRNA release from PP/miRNA and PSSP/miRNA complexes (N/P=15) in the presence of heparin solution.

The miRNA condensing capabilities of PP and PSSP micelles were evaluated by gel retardation assay which could determine whether the miRNA was shielded by polymer or exposed on the surface of the complexes. As Fig.3-A showed, the EtBr fluorescence of the miRNA band gradually disappeared as the PP or PSSP micelles content increased, both PP and PSSP micelles can completely retard DNA at the N/P >6.

RNase protection assay was carried out to investigate whether PP and PSSP micelles could protect miRNA from RNase. As shown in the Fig.3-B, both PP and PSSP micelles could not protect miRNA from RNase's degradation at the N/P=5. But at the N/P=15, both PP and PSSP micelles could protect miRNA compared with naked miRNA which was completely degraded by RNase.

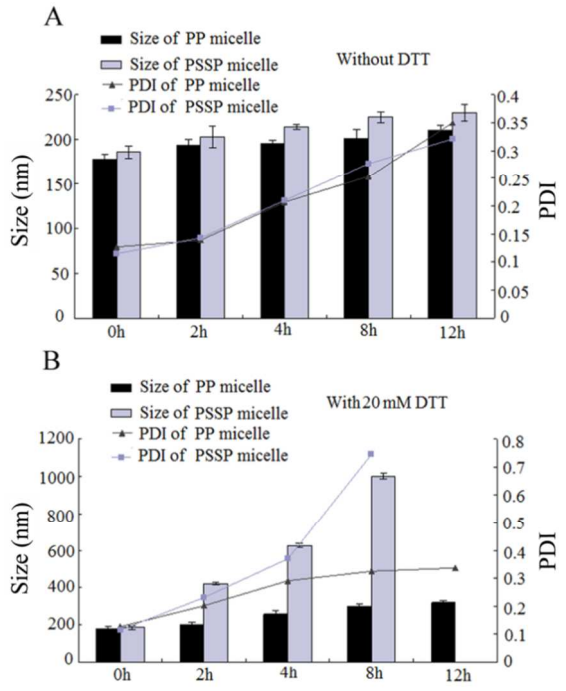

Fig.4. The size and PDI change of PP and PSSP micelles after being treated with 0 mM (A) or 20 mM DTT solution (B) for 0, 2, 4, 8 and 12 h.

The reduction-sensitivity property of the PP and PSSP micelles was monitored for over 24 h by DLS. Fig. 4 shows the size dependence on the incubation time. As shown in the Fig.4-A, the particle size of PP and PSSP micelles treated with blank PBS had no obvious change along with the extended incubation time from 0 h to 24 h, indicating that PP and PSSP were stable in PBS at 37 °C. After the addition of 20 mM DTT which mimics the intracellular redox potential, the size of PSSP micelles increase sharply while no obvious change of the particle sizes was found for PP micelle (Fig.4-B).These data above demonstrated that the stimuli-responsive PSSP micelle was stable in conventional environment and could decompose in reducing environment due to the cleavage of disulfide bond between PCL and PEI. The redox potential-triggering miRNA release from polymer/miRNA complexes was investigated by the gel retardation assay. As shown in Fig.3-C, varies concentrations of heparin could not release any miRNA from the complexes without being treated with 20 mM DTT solution. After being treated by 20 mM DTT, PSSP/miRNA group appeared free miRNA band while PP/miRNA group didn't show any free miRNA band. These data proved that PSSP micelles could protect miRNA in conventional environment and release miRNA successfully at reducing environment.

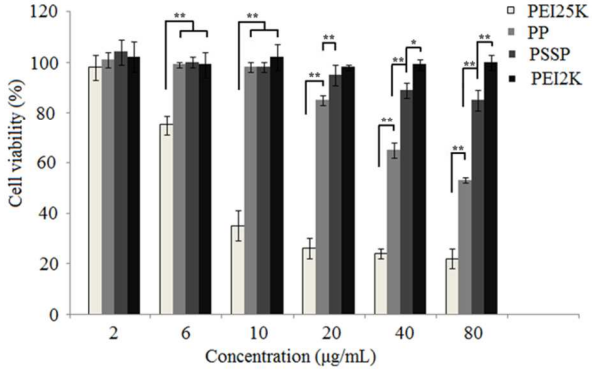

Fig.5. Cytotoxicity of various polymers on B16F10 cell determined by MTT. (n=6, mean ± SD). Incubation time: 24 h. ** and * represent statistically significant difference ($p < 0.01$) and statistically difference ($p < 0.05$) respectively.

The MTT assay was adopted to evaluate the cytotoxicity of PP and PSSP micelles. Fig.5 showed that PP and PSSP micelles exhibited remarkably lower cytotoxicity compared with PEI25K. In general, the cytotoxicity of PEI increased with the rising molecular weight because PEI with high molecular weight aggregated on the cell surface and impaired membrane functions more easily[22]. The molecular weight of PEI2K segment in PP and PSSP were much lower than PEI25K, so the cytotoxicity of PP and PSSP micelles was significantly lower than PEI2K. Both PP and PSSP micelles exhibited higher cytotoxicity than PEI2K at high polymer concentration. The hydrophobic modifications of PEI2K would enhance their adsorption to the cell membrane, aggregation on the cell surface and then increase the cytotoxicity.[23] The toxicity of PSSP micelles was significantly lower than PP micelles as shown in Fig.5 because PSSP micelles could degrade in the intracellular reducing environment and then attenuated its damage to cell treated while PP micelle could not. Above results clearly indicated the low cytotoxicity of PSSP micelles as a potential gene carrier.

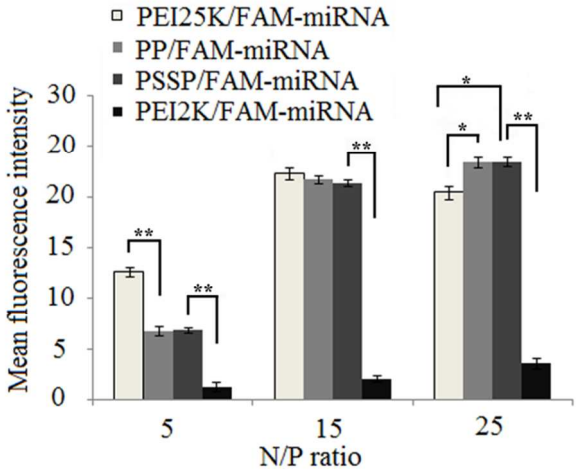

Fig.6.Cellular uptake of Polymer/FAM-miRNA. The mean fluorescence intensity of B16F10 cell treated with different polymer/FAM-miRNA complexes for 4 h measured by flow cytometry. (n=5). ** and * represent statistically significant difference ($p < 0.01$) and statistically difference ($p < 0.05$) respectively.

FITC-labelled miRNA (FAM-miRNA) was used to investigate whether PP and PSSP micelles could help miRNA enter the cells. The cellular uptake of the PP/FAM-miRNA and PSSP/FAM-miRNA complexes was measured by flow cytometry and compared with that of the polyplexes of PEI25K and PEI2K. The influence of N/P ratio on the cellular uptake of the polymer/FAM-miRNA was shown in Fig.6. Increasing the N/P ratio up to 15/1 resulted in enhanced cellular uptake, but there was no further significant increase beyond 15/1. The cellular uptake of PP/FAM-miRNA and PSSP/FAM-miRNA complexes was lower than PEI25K/FAM-miRNA complexes at N/P=5, but the cellular uptake of the three groups was comparable when the N/P increased to 15/1. In addition, the amounts of FAM-miRNA entering the cells in PP/FAM-miRNA and PSSP/FAM-miRNA complexes treated groups were remarkably higher than PEI2K/FAM-miRNA complexes at all N/P ratios. This result could be explained by the hypothesis that the presence of hydrophobic PCL segments in PP and PSSP improved cellular uptake by hydrophobic interactions with the cell membranes.[24, 25] In addition, PP and PSSP micelles could condense miRNA into smaller and more stable nanoscale particles (about 150 nm) compared with PEI2K, providing an

advantage for PP and PSSP micelles to carry miRNA into cell. Besides, Fig.6 showed that PP/FAM-miRNA and PSSP/FAM-miRNA complexes possessed equivalent ability of entering cells, indicating that the introduction of disulfide bonds had no influence on the internalization of miRNA mediated by PCL-PEI copolymer.

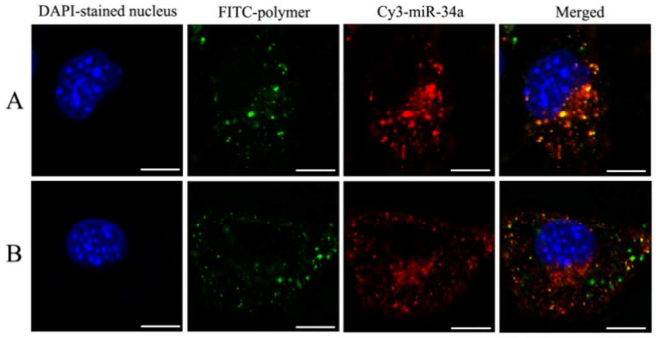

Fig.7. Intracellular distribution of FITC-PP/Cy3-miRNA (A) and FITC-PSSP/Cy3-miRNA (B) complexes at N/P=15. The CLSM observation was performed 4 h after transfection. The scale bar represents 7.5 μm.

The subsequent cytoplasm localization of PP/miRNA and PSSP/miRNA complexes was observed by confocal laser scanning microscope (CLSM) using a multifluorescence-labeling method. As shown in Fig.7, strong green and red fluorescence signal appeared in the cytoplasm of B16F10 cell treated with FITC-PP/Cy3-miRNA complexes and FITC-PSSP/Cy3-miRNA complexes (15/1) after 4 h incubation. After overlapping FITC and Cy3 transmittance channels, lots of yellow spot appeared in the group treated with FITC-PP/Cy3-miRNA, demonstrating that Cy3-miRNA was still associated with the FITC-PP. However, the group treated with FITC-PSSP/Cy3-miRNA complexes had relative fewer yellow spots, which indicated that most of the Cy3-miRNA had been released from the complexes. The stability of the FITC-PSSP/Cy3-miRNA complexes was affected due to the reductive potential in cytoplasm, resulting in the degradation of the micelle and the subsequent release of Cy3-miRNA from the complex. Therefore, PSSP micelles could release more loaded miRNA in cytoplasm than PP micelles.

To evaluate the miRNA delivery efficiencies mediated by PSSP micelles, the endogenous miR-34a was incubated with PSSP micelles to form the PSSP/miR-34a complexes. The PSSP/miR-34a complexes were applied to B16F10 cells, and the cell apoptosis efficiency was compared with that of PEI25K/miR-34a, PP/miR-34a and PEI2K/miR-34a. To exclude the effects of complexes toxicity-mediated damage on the cells, complexation conditions (N/P=15) resulting in low cytotoxicity were adopted. Wound-healing assay was used to evaluate the combined processes of cell migration, cell motility, and proliferation. As shown in Fig.S2, B16F10 cells migrated faster into the nick and the recovery of the wound area was more complete in groups treated with PBS and PEI2K/miR-34a complexes, while PEI25K/miR-34a, PP/miR-34a and PSSP/miR-34a complexes inhibited the wound healing process significantly. These results illustrated that PEI25K/miR-34a, PP/miR-34a and PSSP/miR-34a complexes attenuated the cell motility and migration of tumor cells, but PBS and PEI2K/miR-34a complexes did not show this attenuation effect. As shown in Fig.S2, the group treated with PSSP/miR-34a complexes had worse wound healing ability than the group treated with PP/miR-34a. To evaluate cell apoptosis visually, changes of nucleus morphology were examined by microscope after DAPI staining. The DAPI staining result revealed that extreme chromatin condensation and apoptotic body formation occurred in a greater number of cells in groups treated with PSSP/miR-34a, PP/miR-34a and PEI25K/miR-34a complexes compared with the PBS groups (Fig.S3).

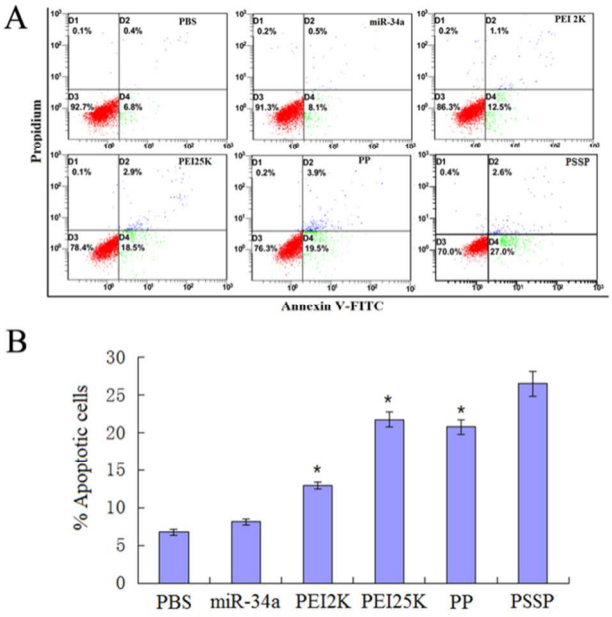

Fig.8. The apoptosis of B16F10cells induced by polymer/miR-34a complexes assayed by flow cytometry.72 h after transfection of the indicated samples, cells were harvested and stained with FITC-Annexin V and propidium iodide (PI) followed by flow cytometric analysis. A: One representative dot plot of each sample. B: Proportion of apoptotic cells after treating with polymer/miR-34a complexes (n = 3).*$p<0.05$ compared with PSSP.

To further investigate the cell apoptosis quantitatively, the number of apoptotic cells was quantified by cytometry after annexin V-FITC and propidium iodide (PI) double-staining. Histograms in Fig.8-A showed that the PSSP/miR-34a group had the highest fraction of cells (27%) in the annexin V^+/PI^- (apoptotic) quadrant, while PEI25k/miR-34a and PP/miR-34a showed less fraction of apoptotic cells (18.5% and 19.5%, respectively). In addition, the subpopulation of PSSP/miR-34a-induced apoptotic cells was significantly larger than that of PP/miR-34a and PEI25K/miR-34a groups ($P < 0.05$;Fig.8-B). These results above suggested that the cell apoptosis effect induced by PSSP/miR-34a complexes is superior to that of PEI25K/miR-34a, PEI2K /miR-34a and PP/miR-34a complexes. The superior cell apoptosis efficiency of PSSP/miR-34a complexes over other polymer/miR-34a complexes could be explained by the intracellular miR-34a distribution status of different complex. The pharmacological effect of miR-34a was essentially determined by the amount of miR-34a distributed in the cytoplasm, the targeting site where the miR-34a could control gene expression efficiently. The cellular uptakes of PSSP/miR-34a and PP/miR-34a complexes were comparable as shown in the cellular uptake study (Fig.6), but the amount of miR-34a released to the cytoplasm was not the same. The CLSM has clearly shown that PSSP/ miRNA could release more miRNA into the cytoplasm than PP/ miRNA (Fig.7).Although PEI25K/miR-34a complex could deliver comparable amount of miR-34a into the cell, the tight packing of genes hindered the releasing of miR-34a into the cytoplasm. Therefore, PSSP/miR-34a complexes could induce more cell apoptosis than PP/miR-34a and PEI25K/miR-34a complexes, which indicated its potential for miRNA delivery.

Conclusions

In summary, gene-condensable and reducible amphiphilic polymer PSSP was synthesized by coupling PCL2K with PEI2K via

a disulfide linkage which can be further assembled into polymeric micelles for miR-34a delivery. PSSP micelles were proven to bind with miRNA. In addition, PSSP micelles were less cytotoxic than PP micelle and PEI25K. The cell apoptosis induced by PSSP/miR-34a complexes was superior to that of PP/miR-34a and PEI25K/miR-34a complexes. Collectively, PSSP micelles represent a promising smart gene vector for effective miRNA delivery. Further research is needed for better understanding and optimization of this delivery system.

Acknowledgements

The financial support from the National Natural Science Foundation of China (No. 81173011, 81422044) and the Science Foundation for Youths of Sichuan Province (No.2012JQ0024) is gratefully acknowledged.

Notes and references

[a] Key Laboratory of Drug Targeting and Drug Delivery Systems, Ministry of Education, West China School of Pharmacy, Sichuan University ChengduNo.17, Section 3, Renmin South Rd, Chengdu, 610041 (P.R. China)

Electronic Supplementary Information (ESI) available. See DOI: 10.1039/c000000x/

1 T. G. Park, J. H. Jeong and S. W. Kim, *Adv Drug Deliv Rev*, 2006, **58**, 467-486.
2 M. Neu, D. Fischer and T. Kissel, *J Gene Med*, 2005, **7**, 992-1009.
3 M. Ohsaki, T. Okuda, A. Wada, T. Hirayama, T. Niidome and H. Aoyagi, *Bioconjug Chem*, 2002, **13**, 510-517.
4 W. T. Godbey, K. K. Wu and A. G. Mikos, *Biomaterials*, 2001, **22**, 471-480.
5 B. Liang, M. L. He, C. Y. Chan, Y. C. Chen, X. P. Li, Y. Li, D. Zheng, M. C. Lin, H. F. Kung, X. T. Shuai and Y. Peng, *Biomaterials*, 2009, **30**, 4014-4020.
6 H. H. Ahn, J. H. Lee, K. S. Kim, J. Y. Lee, M. S. Kim, G. Khang, I. W. Lee and H. B. Lee, *Biomaterials*, 2008, **29**, 2415-2422.
7 H. Y. Tian, C. Deng, H. Lin, J. Sun, M. Deng, X. Chen and X. Jing, *Biomaterials*, 2005, **26**, 4209-4217.
8 K. Kono, H. Akiyama, T. Takahashi, T. Takagishi and A. Harada, *Bioconjug Chem*, 2005, **16**, 208-214.
9 C. Arigita, N. J. Zuidam, D. J. Crommelin and W. E. Hennink, *Pharm Res*, 1999, **16**, 1534-1541.
10 A. U. Bielinska, J. F. Kukowska-Latallo and J. R. Baker, Jr., *Biochim Biophys Acta*, 1997, **1353**, 180-190.
11 Y. H. Kim, J. H. Park, M. Lee, T. G. Park and S. W. Kim, *J Control Release*, 2005, **103**, 209-219.
12 D. Soundara Manickam and D. Oupicky, *J Drug Target*, 2006, **14**, 519-526.
13 F. Meng, W. E. Hennink and Z. Zhong, *Biomaterials*, 2009, **30**, 2180-2198.
14 Y. Lee, H. Mo, H. Koo, J. Y. Park, M. Y. Cho, G. W. Jin and J. S. Park, *Bioconjug Chem*, 2007, **18**, 13-18.
15 R. Garzon, G. Marcucci and C. M. Croce, *Nat Rev Drug Discov*, 2010, **9**, 775-789.
16 K. Kojima, Y. Fujita, Y. Nozawa, T. Deguchi and M. Ito, *Prostate*, 2010, **70**, 1501-1512.
17 Y. Akao, S. Noguchi, A. Iio, K. Kojima, T. Takagi and T. Naoe, *Cancer Lett*, 2011, **300**, 197-204.
18 L. Y. Qiu and Y. H. Bae, *Biomaterials*, 2007, **28**, 4132-4142.
19 J. X. Zhang, L. Y. Qiu, Y. Jin and K. J. Zhu, *J Biomed Mater Res A*, 2006, **76**, 773-780.
20 S. Emanuele, M. Lauricella, D. Carlisi, B. Vassallo, A. D'Anneo, P. Di Fazio, R. Vento and G. Tesoriere, *Apoptosis*, 2007, **12**, 1327-1338.
21 S. Shi, L. Han, T. Gong, Z. Zhang and X. Sun, *Angew Chem Int Ed Engl*, 2013, **52**, 3901-3905.
22 D. Fischer, Y. Li, B. Ahlemeyer, J. Krieglstein and T. Kissel, *Biomaterials*, 2003, **24**, 1121-1131.
23 Z. Liu, J. Janzen and D. E. Brooks, *Biomaterials*, 2010, **31**, 3364-3373.
24 Z. Liu, Z. Zhang, C. Zhou and Y. Jiao, *Prog Polym Sci*, 2010, **35**, 1144-1162.
25 S. Y. Wong, J. M. Pelet and D. Putnam, *Prog Polym Sci*, 2007, **32**, 799-837.

